


Article

Dominant Contributions of Secondary Aerosols and Vehicle Emissions to Water-Soluble Inorganic Ions of PM_{2.5} in an Urban Site in the Metropolitan Hangzhou, China

Chun Xiong ¹, Shaocai Yu ^{1,2,*}, Xue Chen ¹, Zhen Li ¹, Yibo Zhang ¹, Mengying Li ¹, Weiping Liu ¹ , Pengfei Li ^{3,*} and John H. Seinfeld ²

¹ Research Center for Air Pollution and Health, Key Laboratory of Environmental Remediation and Ecological Health, Ministry of Education, College of Environmental and Resource Sciences, Zhejiang University, Hangzhou 310058, China; 21614014@zju.edu.cn (C.X.); cxoldsnow@zju.edu.cn (X.C.); lizhen1942@163.com (Z.L.); ybzhzhang903@zju.edu.cn (Y.Z.); 11814019@zju.edu.cn (M.L.); wliu@zju.edu.cn (W.L.)

² Division of Chemistry and Chemical Engineering, California Institute of Technology, Pasadena, CA 91125, USA; seinfeld@caltech.edu

³ College of Science and Technology, Hebei Agricultural University, Baoding 071000, China

* Correspondence: shaocaiyu@zju.edu.cn (S.Y.); lpf_zju@163.com (P.L.)

Abstract: Water soluble inorganic ions (WSIIs) are important components in PM_{2.5} and could strongly affect the acidity and hygroscopicity of PM_{2.5}. In order to achieve the seasonal characteristics and determine the potential sources of WSIIs in PM_{2.5} in Hangzhou, online systems were used to measure hourly mass concentrations of WSIIs (SO₄^{2−}, NO₃[−], NH₄⁺, Cl[−], Na⁺, K⁺, Ca²⁺ and Mg²⁺) as well as PM_{2.5}, NO₂ and SO₂ at an urban site for one month each season (May, August, October, December) in 2017. Results showed that the hourly mass concentrations of PM_{2.5} during the whole campaign varied from 1 to 292 μg·m^{−3} with the mean of 56.03 μg·m^{−3}. The mean mass concentration of WSIIs was 26.49 ± 20.78 μg·m^{−3}, which contributed 48.28% to averaged PM_{2.5} mass. SNA (SO₄^{2−}, NO₃[−] and NH₄⁺) were the most abundant ions in PM_{2.5} and on average, they comprised 41.57% of PM_{2.5} mass. PM_{2.5}, NO₂, SO₂ and WSIIs showed higher mass concentrations in December, possibly due to higher energy consumption emissions, unfavorable meteorological factors (e.g., lower wind speed and temperature) and regional transport. Results from PCA models showed that secondary aerosols and vehicle emissions were the dominant sources of WSIIs in the observations. Our findings highlight the importance of stronger controls on precursor (e.g., SO₂ and NO₂) emissions in Hangzhou, and show that industrial areas should be controlled at local and regional scales in the future.

Keywords: secondary aerosols; vehicle emissions; water-soluble inorganic ions; HYSPLIT model; Hangzhou



Citation: Xiong, C.; Yu, S.; Chen, X.; Li, Z.; Zhang, Y.; Li, M.; Liu, W.; Li, P.; Seinfeld, J.H. Dominant Contributions of Secondary Aerosols and Vehicle Emissions to Water-Soluble Inorganic Ions of PM_{2.5} in an Urban Site in the Metropolitan Hangzhou, China.

Atmosphere **2021**, *12*, 1529. <https://doi.org/10.3390/atmos12111529>

Academic Editor: Ashok Kumar

Received: 14 October 2021

Accepted: 14 November 2021

Published: 19 November 2021

Publisher's Note: MDPI stays neutral with regard to jurisdictional claims in published maps and institutional affiliations.



Copyright: © 2021 by the authors. Licensee MDPI, Basel, Switzerland. This article is an open access article distributed under the terms and conditions of the Creative Commons Attribution (CC BY) license (<https://creativecommons.org/licenses/by/4.0/>).

1. Introduction

Due to rapid urbanization and industrialization during the decades, Chinese metropolitan cities suffered from heavy air pollution that was mainly caused by high PM_{2.5} concentrations [1–4]. PM_{2.5} (particulate matters less than 2.5 μm in aerodynamic diameter), originating from both direct emissions and secondary transformations, could strongly affect physical health [5–7], air quality [8,9] and radiative forcing [10,11]. For sustainable developments, reducing PM_{2.5} concentration levels had become one of the most urgent issues in China. In order to alleviate air pollution, the Chinese government released a series of strong and rigorous regulations since 2013 (e.g., “Air Pollution Prevention and Control Action Plan”) and PM_{2.5} levels in many polluted cities were reported to decrease considerably [12,13]. Nonetheless, PM_{2.5} concentrations still exceeded the corresponding Chinese National Ambient Air Quality Standard (CNAQS) in many cities [14–18].

PM_{2.5} comprises a variety of components such as water-soluble inorganic ions (WSIIs). WSIIs accounted for more than one-third of PM_{2.5} mass [19] and can significantly affect the characteristics of PM_{2.5} [20] by existing in specific forms. For example, NH₄NO₃ and (NH₄)₂SO₄ were found to be two important forms in PM_{2.5} and higher mass fractions of which could make PM_{2.5} more hygroscopic in the atmosphere, thus leading to degradation of visibility [21,22]. Moreover, WSIIs can also affect the acidity of PM_{2.5}, and heterogeneous chemical reactions on surfaces of fine particles [23,24].

Hangzhou is the capital city of the Zhejiang province and it is located in east of the YRD area. Cities surrounding Hangzhou include the megacity of Shanghai in the northeast and highly industrialized cities such as Suzhou, Wuxi, and Changzhou in the north and Ningbo in the southeast. Hangzhou belongs to the subtropical zone with a humid monsoon climate, characterized by a prevailing southeasterly wind in summer and northwesterly wind in winter [25]. The Gross Domestic Product in Hangzhou was 1255.6 billion in 2017, increasing by 50.50% from 2013 [26]. However, with the rapid growth, Hangzhou suffered from severe air pollution. For example, during the heavy haze period in the winter of 2013, most of PM_{2.5} hourly concentrations were higher than 200 µg·m⁻³ with the highest concentration of 588 µg·m⁻³, largely exceeding the CNAAQs [22].

While there were many observations of WSIIs in Hangzhou [27–33], most studies focused on pollution episodes in one or two seasons [30–32] and seasonal observations in Hangzhou were rare. Moreover, many long-term studies of WSIIs employing offline analytical methods with filter-based sampling may have the drawbacks of low time resolution and mass losses owing to semi-volatile aerosol evaporation [34,35]. Thus, in this study, we used on-line Monitoring of AeRosols and Gases (MARGA 1S, Applikon Analytical B. V. Corp., The Netherlands) to measure hourly concentrations of WSIIs during one month for each season at an urban site in Hangzhou. Simultaneously, hourly concentrations of PM_{2.5}, NO₂, and SO₂ were also measured to analyze ionic reactions. Here, we first give detailed descriptions of the levels of PM_{2.5} and WSIIs during observation. Then, we use back trajectory analyses, cluster analyses and principal component analyses (PCA) to determine sources of WSIIs during four months of sampling. The object of the study is to give scientific insights into seasonal variations and potential sources of WSIIs of PM_{2.5}, providing scientific basis for air pollution controls in Hangzhou.

2. Experiment

2.1. Instruments

Hourly average concentrations of NO₂, SO₂, and PM_{2.5} were measured with a model 42i NO₂ analyzer, model 43i SO₂ analyzer and TEOM 1405F-FDMS (Thermo Fisher Scientific, Co., Ltd., Waltham, MA, USA), respectively. These instruments underwent external calibration four times a year. Meteorological factors (relative humid, temperature, wind speed, wind direction, rainfall) were measured by automatic weather station (Vaisala WXT520).

WSIIs were measured by Monitoring of AeRosols and Gases (MARGA 1S, Applikon Analytical B. V. Corp., Schiedam, The Netherlands) with hourly time resolution. The MARGA 1S system comprises a sampling box and an analytic box. Ambient air is first drawn through a PM_{2.5} size selecting inlet (flow rate: 1 m³·h⁻¹) by an air pump controlled by a Mass Flow Controller (MFC). After that, air flows pass through a Wet Rotating Denuder (WRD) and the trace gases can be removed by 0.0035% H₂O₂ liquid film in WRD. Particles can directly pass the WRD with air flow and then grow by a deliquescence progress and be captured in a Steam Jet Aerosol Collector (SJAC), within which a supersaturated environment was created by a streamer (120–140 °C). After degassing progresses and mixing with internal standard solutions (LiBr, Li⁺ was the internal standard for cations' analyses and Br⁻ was the internal standard for anions' analyses), the WRD sample liquid will be transported by syringes and finally analyzed by Ion Chromatographic (IC). The MARGA 1S system has the capability of measuring hourly averaged aerosol concentrations of major WSIIs (SO₄²⁻, NO₃⁻, NH₄⁺, Cl⁻, Na⁺, K⁺, Ca²⁺, Mg²⁺). The detection limits of the

MARGA 1S system were $0.001 \mu\text{g}\cdot\text{m}^{-3}$ for Cl^- , $0.005 \mu\text{g}\cdot\text{m}^{-3}$ for NO_3^- , $0.004 \mu\text{g}\cdot\text{m}^{-3}$ for SO_4^{2-} , $0.005 \mu\text{g}\cdot\text{m}^{-3}$ for NH_4^+ , $0.005 \mu\text{g}\cdot\text{m}^{-3}$ for Na^+ , $0.009 \mu\text{g}\cdot\text{m}^{-3}$ for K^+ , $0.006 \mu\text{g}\cdot\text{m}^{-3}$ for Mg^{2+} , $0.009 \mu\text{g}\cdot\text{m}^{-3}$ for Ca^{2+} . More details of the MARGA 1S system can be found elsewhere [36].

2.2. Site

The observation site was located in Zijingang Campus of Zhejiang University in Hangzhou, China (30.31° N , 120.08° E). MARGA 1S system, model 42i NO_2 analyzer, model 43i SO_2 analyzer and TEOM 1405F-FDMS were located in a measurement container, within which the temperature was maintained at $\sim 25^\circ \text{ C}$. Sample Inlets of the MARGA 1S system, model 42i NO_2 analyzer, model 43i SO_2 analyzer and TEOM 1405F-FDMS were located at the roof of the container. Around 700 m in the north side away from the sample site was a main road. Student dormitories were around 500 m away from the site on the east side. Construction areas were around 400 m from the site to the west and north. The observation site was influenced by a combination of traffic, residences, and construction and thus could well represent the urban area [37].

$\text{PM}_{2.5}$, SO_2 , NO_2 and WSIs were measured during one month per season in 2017: May in spring, August in summer, October in autumn and December in winter.

2.3. Methods

2.3.1. Back Trajectory and Clusters Analysis

Based on the National Ocean and Atmospheric Administration (NOAA) Hybrid Single-Particle Lagrangian Integrated Trajectory (HYSPPLIT) model (<http://ready.arl.noaa.gov/HYSPPLIT.php>, accessed on 29 July 2021), an open source software (TrajStat, Version 1.2.2.6) was used to calculate the backward air mass trajectories arriving at our site to determine the regional transport of pollutants [38,39]. Inputs were Global Data Assimilation System (GDAS) meteorological data at a grid resolution of $1^\circ \times 1^\circ$ [22].

In this study, 72 h back trajectories run 4 times a day (i.e., with ending time at 0:00, 6:00, 12:00, 18:00, local time) ending at the arrival level of 100 m from the measured site. The concentrations of pollutants (e.g., $\text{PM}_{2.5}$) were associated with the corresponding trajectory [40]. By using a K-means clustering algorithm, air mass trajectories were assigned in different clusters [39,40].

2.3.2. Principal Component Analysis

Principal component analysis (PCA) method can reduce the dimensionality of a data set effectively [41]. In this study, the PCA model was used to determine sources of WSIs during four months of sampling. When assuming liner relationships between the contributions of each source and concentrations of pollutants, a pollutant data matrix $\{C_{ij}\}$ can convert to dimensionless standardized form $\{S_{ij}\}$ using the following formula [42]:

$$\{C_{ij}\} = \begin{Bmatrix} C_{11} & \cdots & C_{1n} \\ \vdots & \vdots & \vdots \\ C_{m1} & \cdots & C_{mn} \end{Bmatrix} \quad (1)$$

$$\{S_{ij}\} = \left\{ \frac{C_{ij} - d_j}{\sigma_j} \right\} \quad (2)$$

where m and n are number of total hours (i.e., lines of $\{C_{ij}\}$) of the input observation data and total number of pollutants' species (i.e., columns of $\{C_{ij}\}$), respectively. C_{ij} represents concentration of hour i and pollutant j . σ_j and d_j are the standard deviation and mathematic average value of pollutant, j , respectively. Then, the covariance matrix of standardized $\{S_{ij}\}$ and the corresponding eigenvalues and eigenvectors of the covariance matrix were calculated by applying eigenvector decomposition. The eigenvector with higher corresponding eigenvalue could account for the larger proportion of variability and cover more

information of original $\{C_{ij}\}$ [41]. After performing the above procedures, $C\{S_{ij}\}$ could finally be expressed as the equation below:

$$\{S_{ij}\} = \left\{ \sum_{l=1}^k a_{il} b_{lj} \right\} \quad (3)$$

where k is the number of total sources and $l = 1, 2, \dots, k$. a_{il} and b_{lj} are the factor loadings and scores [42], respectively.

In this study, all species of WSIs in four seasons observed by MARGA were used in the PCA calculations performed by SPSS software (version 23.0, corporation of IBM).

2.4. Quality Assurance/Quality Control

The MARGA 1S system was well calibrated twice a year with external blank and at least 4 individual standard solutions with different concentrations. The concentration ranges of WSIs for calibrations were 6 ppb~600 ppb for Cl^- , 20 ppb~400 ppb for Br^- , 20 ppb~2000 ppb for NO_3^- , 30 ppb~3000 ppb for SO_4^{2-} , 20 ppb~400 ppb for Li^+ , 20 ppb~400 ppb for Na^+ , 25 ppb~500 ppb for NH_4^+ , 50 ppb~1000 ppb for K^+ , 25 ppb~500 ppb for Mg^{2+} and 50 ppb~1000 ppb for Ca^{2+} . The correlation coefficients (R^2) of calibration curves were all above 0.98. Outliers and concentrations of WSIs that below minimum detection limit were removed before the PCA analysis. The percentages of valid data of all WSIs were above 90% except for Mg^{2+} which was above 85%.

The concentrations of internal standard solutions (Br^- and Li^+) were varied within mean concentration ± 3 standard deviations during the whole observations, ensuring the stability and accuracy of data for the whole observations.

3. Results and Discussions

3.1. SO_2 , NO_2 and $\text{PM}_{2.5}$ Levels

Table 1 shows the mean concentrations of SO_2 , NO_2 and $\text{PM}_{2.5}$ in Hangzhou as well as other cities in China. The concentrations of SO_2 in Hangzhou varied from 2 to $39 \mu\text{g}\cdot\text{m}^{-3}$ with the mean of $7.95 \mu\text{g}\cdot\text{m}^{-3}$, which was notably lower than those in Handan ($37.2 \mu\text{g}\cdot\text{m}^{-3}$) in 2017. Higher energy consumptions and higher emission industries in Handan than those in Hangzhou may be the main cause [14]. The mean concentration of SO_2 in our study was slightly higher than that in Shanghai ($7 \mu\text{g}\cdot\text{m}^{-3}$) in 2013~2014, partly due to better diffusional conditions in the coastal cities (e.g., Shanghai). The concentrations of NO_2 in 2017 in Hangzhou varied from 3 to $120 \mu\text{g}\cdot\text{m}^{-3}$ with the mean of $36.49 \mu\text{g}\cdot\text{m}^{-3}$, which was largely higher than those in Hangzhou ($23 \mu\text{g}\cdot\text{m}^{-3}$) in 2013~2014. The car ownership was around 2.79 million in 2017 and 2.54 million in 2013 [26] in Hangzhou, respectively, thus the increasing trend of NO_2 annual concentration could be attributed to the growth of automobile population in Hangzhou.

Table 1. The mean concentrations of SO_2 , NO_2 and $\text{PM}_{2.5}$ in Hangzhou and other cities.

City	Time	Mean Concentration ($\mu\text{g}\cdot\text{m}^{-3}$)			Reference
		SO_2	NO_2	$\text{PM}_{2.5}$	
Handan	2017	37.2	51.7	85.7	[14]
Nanning	2017/09~2018/08	11	36	36	[43]
Chengdu	2016	16	43	65	[44]
Guangzhou	2017	10.11	52.27	31.59	[45]
Wuhan	2013/03~2014/02	32.4	54.9	89.6	[46]
Zhengzhou	2017~2018	20.5	51.6	70.5	[16]
Xinxiang	2017~2018	23.8	51.4	69.0	[16]
Shanghai	2013/03~2014/02	7	20	56	[47]
Hangzhou	2013/03~2014/02	9	23	64	[47]
Hangzhou	2017/05,08,10,12	7.95	36.49	56.03	This study

The concentrations of PM_{2.5} in the field ranged from 1 to 292 $\mu\text{g}\cdot\text{m}^{-3}$ with a mean of 56.03 $\mu\text{g}\cdot\text{m}^{-3}$, which exceeded Chinese National Ambient Air Quality Standard grade II (35 $\mu\text{g}\cdot\text{m}^{-3}$). The mean concentration in this study was lower than those in Handan (85.7 $\mu\text{g}\cdot\text{m}^{-3}$), Chengdu (65 $\mu\text{g}\cdot\text{m}^{-3}$), Wuhan (89.6 $\mu\text{g}\cdot\text{m}^{-3}$), Zhengzhou (70.5 $\mu\text{g}\cdot\text{m}^{-3}$) and Xinxiang (69.0 $\mu\text{g}\cdot\text{m}^{-3}$), similar to that in Shanghai (56 $\mu\text{g}\cdot\text{m}^{-3}$), but higher than those in Nanning (36 $\mu\text{g}\cdot\text{m}^{-3}$) and Guangzhou (31.59 $\mu\text{g}\cdot\text{m}^{-3}$) (Table 1). As shown in Table 1, PM_{2.5} mean concentration dropped from 2013–2014 to 2017 in Hangzhou. This could be attributed to the implementation of stringent emission control measures during the period 2013–2017 in China [14]. However, the annual PM_{2.5} concentrations were still 1.60 times the Chinese National Ambient Air Quality Standard of PM_{2.5} (35 $\mu\text{g}\cdot\text{m}^{-3}$), indicating that air pollution was still severe in Hangzhou.

As shown in Table 2, PM_{2.5} showed obvious variations in Hangzhou in four months. PM_{2.5} mean concentrations were the highest in December (89.35 \pm 40.21 $\mu\text{g}\cdot\text{m}^{-3}$), followed by May (58.39 \pm 26.00 $\mu\text{g}\cdot\text{m}^{-3}$), October (47.26 \pm 26.05 $\mu\text{g}\cdot\text{m}^{-3}$) and August (26.30 \pm 13.55 $\mu\text{g}\cdot\text{m}^{-3}$). The lowest PM_{2.5} concentrations, in August, were due to the highest wind speed (1.45 \pm 0.71 $\text{m}\cdot\text{s}^{-1}$) and temperature (30.14 \pm 3.76 $^{\circ}\text{C}$), which were favorable factors for the diffusion of pollutants. The highest concentrations of precursors SO₂ (12.57 \pm 5.37 $\mu\text{g}\cdot\text{m}^{-3}$) and NO₂ (50.20 \pm 17.35 $\mu\text{g}\cdot\text{m}^{-3}$) also occurred in the December, indicating more energy consumption and pollutant emissions. Additionally, the lowest wind speeds and temperatures also occurred in December, resulting in the accumulation of pollutants.

Table 2. The mean (mean \pm standard deviation) of meteorological factors, concentrations of gases and WSIs.

	Mean \pm SD				
	May	August	October	December	Mean
Meteorological factors					
RH (%)	70.58 \pm 22.00	71.95 \pm 17.06	76.82 \pm 17.32	71.17 \pm 23.34	72.62 \pm 20.26
T ^a ($^{\circ}\text{C}$)	22.73 \pm 4.73	30.14 \pm 3.76	18.82 \pm 4.58	6.77 \pm 4.14	19.62 \pm 9.49
WS ^b ($\text{m}\cdot\text{s}^{-1}$)	1.40 \pm 0.75	1.45 \pm 0.71	1.36 \pm 0.70	1.04 \pm 0.64	1.31 \pm 0.72
Concentrations of gases ($\mu\text{g}\cdot\text{m}^{-3}$)					
SO ₂	7.70 \pm 3.37	4.59 \pm 1.58	6.98 \pm 3.37	12.57 \pm 5.37	7.95 \pm 4.67
NO ₂	39.55 \pm 17.99	20.23 \pm 10.38	36.13 \pm 15.96	50.20 \pm 17.35	36.49 \pm 19.02
Concentrations of PM _{2.5} and WSIs ($\mu\text{g}\cdot\text{m}^{-3}$)					
PM _{2.5}	58.39 \pm 26.00	26.30 \pm 13.55	47.26 \pm 26.05	89.35 \pm 40.21	56.03 \pm 36.35
Cl [−]	0.68 \pm 0.69	0.32 \pm 0.21	0.98 \pm 0.60	2.65 \pm 1.43	1.07 \pm 1.33
NO ₃ [−]	8.38 \pm 6.93	2.12 \pm 1.92	10.26 \pm 8.44	20.62 \pm 12.15	9.86 \pm 10.75
SO ₄ ^{2−}	9.22 \pm 3.94	5.48 \pm 3.98	7.35 \pm 5.05	9.36 \pm 5.93	7.57 \pm 4.99
NH ₄ ⁺	5.80 \pm 3.10	2.76 \pm 1.85	5.54 \pm 4.18	10.50 \pm 6.43	5.86 \pm 4.91
Na ⁺	0.19 \pm 0.11	0.17 \pm 0.10	0.23 \pm 0.16	0.37 \pm 0.18	0.23 \pm 0.16
K ⁺	0.75 \pm 0.61	0.23 \pm 0.11	0.40 \pm 0.24	0.94 \pm 0.54	0.45 \pm 0.47
Ca ²⁺	0.32 \pm 0.35	0.16 \pm 0.08	0.19 \pm 0.17	0.61 \pm 0.47	0.27 \pm 0.30
Mg ²⁺	0.06 \pm 0.04	0.05 \pm 0.03	0.08 \pm 0.04	0.09 \pm 0.08	0.08 \pm 0.10
Calculations					
Sum ^c ($\mu\text{g}\cdot\text{m}^{-3}$)	25.40 \pm 13.10	11.10 \pm 6.91	24.88 \pm 17.23	44.78 \pm 24.75	26.49 \pm 20.78
Percentage ^d (%)	47.48 \pm 16.62	43.37 \pm 16.01	51.85 \pm 14.10	49.62 \pm 13.54	48.28 \pm 15.33

^a Temperature. ^b Wind speed. ^c sum of WSIs. ^d mean value of sum of WSIs divided by mean concentration of PM_{2.5}.

3.2. WSIs in PM_{2.5}

As shown in Table 2, the mean WSIs concentration in PM_{2.5} was $26.49 \pm 20.78 \mu\text{g}\cdot\text{m}^{-3}$, which contributed $48.28 \pm 15.33\%$ to PM_{2.5} concentrations. The contribution was notably higher than that in Taiyuan (32.86%) [48], but lower than that in Nanning (51.65%) [43]. The concentrations of WSIs in PM_{2.5} from high to low were NO_3^- ($9.86 \pm 10.75 \mu\text{g}\cdot\text{m}^{-3}$), SO_4^{2-} ($7.57 \pm 4.99 \mu\text{g}\cdot\text{m}^{-3}$), NH_4^+ ($5.86 \pm 4.91 \mu\text{g}\cdot\text{m}^{-3}$), Cl^- ($1.07 \pm 1.33 \mu\text{g}\cdot\text{m}^{-3}$), K^+ ($0.45 \pm 0.47 \mu\text{g}\cdot\text{m}^{-3}$), Ca^{2+} ($0.27 \pm 0.30 \mu\text{g}\cdot\text{m}^{-3}$), Na^+ ($0.23 \pm 0.16 \mu\text{g}\cdot\text{m}^{-3}$), and Mg^{2+} ($0.08 \pm 0.10 \mu\text{g}\cdot\text{m}^{-3}$). On average, the SNA (SO_4^{2-} , NO_3^- and NH_4^+) concentrations were $23.29 \mu\text{g}\cdot\text{m}^{-3}$ in sum, contributing 91.73% and 41.57% to WSIs and PM_{2.5}, respectively. The mean concentration of SNA was lower than that in Zhengzhou ($28.4 \mu\text{g}\cdot\text{m}^{-3}$) and in Xinxiang ($29.6 \mu\text{g}\cdot\text{m}^{-3}$) in 2017~2018 [16]. However, the mean contribution of SNA to PM_{2.5} concentrations in Hangzhou were notably higher than that in Zhengzhou (23.8%) and in Xinxiang (23.0%) [16]. This may due to the higher RH in Hangzhou (72.62%) than those in Zhengzhou (62.6%) and in Xinxiang (60.9%) as the higher RH could enlarge the sizes of particle matters, thus facilitating the absorption of NO_2 and SO_2 on the aerosol surfaces through heterogeneous formations of nitrates and sulfates [14].

Figure 1 shows the mean variations of PM_{2.5}, SO_4^{2-} , NO_3^- and NH_4^+ in this study, as well as previous studies in Hangzhou [27,28], as well as comparing these with measurements at Handan, a typical polluted city in the North China Plain, during similar a period [14]. As shown in Figure 1, annual concentrations of PM_{2.5} decreased by -26.06% from the periods of April 2004~March 2005 ($108.2 \mu\text{g}\cdot\text{m}^{-3}$) to December 2014~November 2015 ($80.0 \mu\text{g}\cdot\text{m}^{-3}$) and then continuously decreased by -35.43% to 2017 ($56.03 \mu\text{g}\cdot\text{m}^{-3}$) (this study). Annual concentrations of SO_4^{2-} and NH_4^+ also showed a decreasing trend. Such remarkable reductions could be attributed to the implementation of stringent emission control measures, especially on emissions of combustions of traditional fossil fuel [17,49]. NO_3^- showed a different trend, rising from $8.3 \mu\text{g}\cdot\text{m}^{-3}$ (April 2004~March 2005) to $14.2 \mu\text{g}\cdot\text{m}^{-3}$ (December 2014~November 2015) and then decreasing to $9.86 \mu\text{g}\cdot\text{m}^{-3}$ in 2017. This may due to the increasing automobile population. The automobile population was 0.41 million in the year of 2004, and it notably increased to 2.54 million in 2013 [26], resulting in higher annual NO_3^- concentrations in December 2014~November 2015. Though the automobile population was 2.79 million in 2017 and was higher than that of 2013 [26], the implementation of stringent emission control measures since 2013 could be the main cause of the reduction in NO_3^- . The most abundant ion among WSIs was SO_4^{2-} during April 2004~March 2005, but this changed to NO_3^- during December 2014~November 2015 and remained unchanged in 2017, highlighting the strong influence of motor vehicles on the chemical characteristics of PM_{2.5} in Hangzhou city. As for Handan city, where more high emission industries were located [14], the average PM_{2.5}, SO_4^{2-} , NO_3^- , NH_4^+ concentrations were 1.66 times, 1.70 times, 1.33 times and 1.45 times higher than those in Hangzhou in 2017, respectively.

The average SNA/PM_{2.5} value was 32.0% during April 2004~March 2005 (calculated by SNA and PM_{2.5} average concentrations in [28]). Notably, it increased 1.39-fold to 44.5% in 2014~2015 [27] and then generally stayed stable in 2017 (41.57%) (this study), indicating the increase contributions of secondary reactions to PM_{2.5} in Hangzhou. SNA/PM_{2.5} ratios in Handan were 40.4% , lower than those in this study, representing a lower contribution of secondary transformations to PM_{2.5} in Handan. As discussed above, this is partly due to higher RH on average in Hangzhou than in Handan because higher RH could promote liquid and heterogeneous reactions, resulting in the increased formations of SNA [14].

WSIs values showed obvious variations during the four sampling months in Hangzhou. As shown in Table 2, the mean concentrations of Cl^- in December were the highest, being 8.28 times higher than those in August because of enhanced emissions from coal combustion in winter. The concentrations of K^+ were higher in December and May. This can be attributed to biomass burning in May and December, since K^+ is a dominant ion from biomass burning [50]. This differed from Beijing, where concentrations of K^+ were found to be the highest in autumn [19]. SO_4^{2-} is commonly believed to be a crucial

ion in WSIs and is mainly produced by photochemical oxidations of sulfur-containing precursors [51]. In this study, SO_4^{2-} showed low concentration levels and minor changes in four sampling months. On the other hand, NO_3^- indicated strong variations, with the mean concentrations in December being 9.73 times higher than those in August. Strong volatility of nitrate (e.g., NH_4NO_3) under high temperature conditions can be a possible reason for low concentrations of NO_3^- in August, whereas the high NO_2 concentration in December may intensify the production of NO_3^- . NH_4^+ could result from fertilizers and conversion from NH_3 and be affected by aerosol acidity, temperature and water availability [52]. In this study, the variation order of NH_4^+ from low to high is December > October > May > August. Ca^{2+} , as an important indicator of dust, showed very low concentrations in the observation.

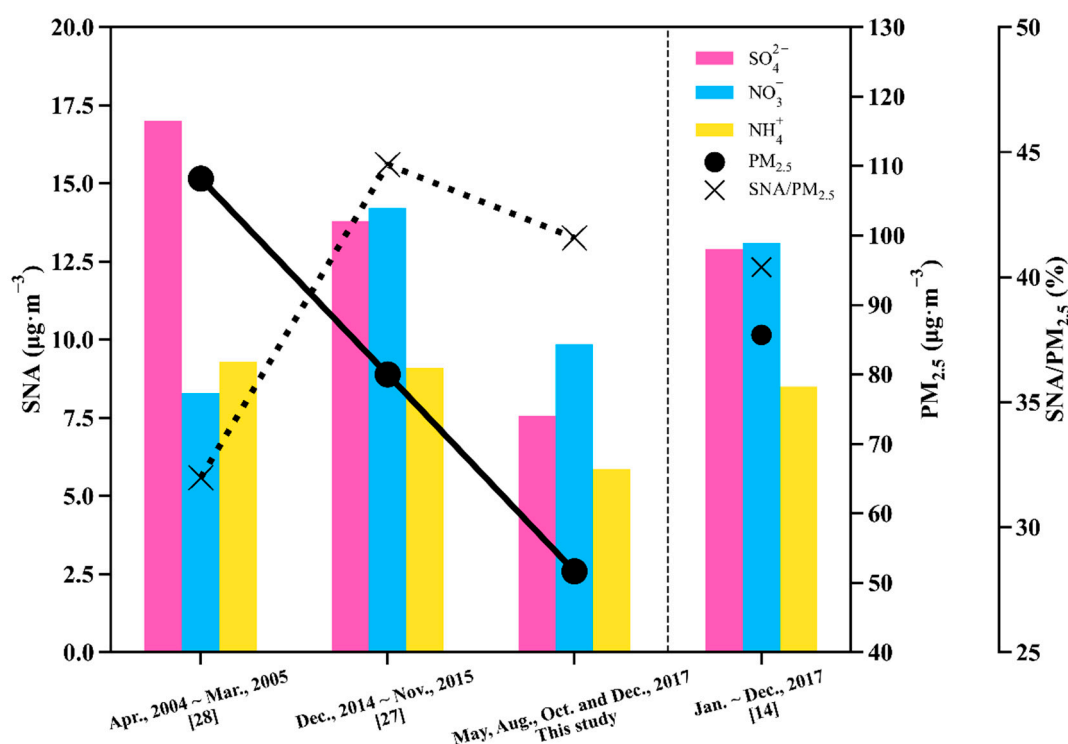


Figure 1. Comparisons of concentrations of $\text{PM}_{2.5}$ and WSIs with previous results in the cities of Hangzhou and Handan.

3.3. Acidity

We used ion balance calculations to investigate the $\text{PM}_{2.5}$ acidities, which can be strongly influenced by the equivalence of WSIs. Here, two equations (Anion Equivalence and Cation Equivalence) were used for calculating the balance between anions and cations as follows:

- (1) Cation Equivalence (CE) = $[\text{NH}_4^+] + [\text{Na}^+] + [\text{K}^+] + 2[\text{Mg}^{2+}] + 2[\text{Ca}^{2+}]$
- (2) Anion Equivalence (AE) = $[\text{NO}_3^-] + 2[\text{SO}_4^{2-}] + [\text{Cl}^-]$ where the concentrations of WSIs ($\mu\text{g}\cdot\text{m}^{-3}$) were converted into micro-equivalents ($\mu\text{mol}\cdot\text{m}^{-3}$) in the above two equations.

As illustrated by the scatter plots in Figure 2, strong correlations existed between CE vs. AE . The slopes of correlation equations in May (Figure 2a), August (Figure 2b), October (Figure 2c), and December (Figure 2d) were 1.00, 1.03, 1.01, and 1.11, respectively, revealing a slightly basic trend and a deficiency in anions ($\text{CE}/\text{AE} > 1$) in the $\text{PM}_{2.5}$ samples. Good correlations existed between $[\text{NH}_4^+]$ vs. $([\text{NO}_3^-] + 2[\text{SO}_4^{2-}] + [\text{Cl}^-])$ with the slopes of 0.96 (May), 1.00 (August), 0.99 (October), and 1.08 (December), revealing that anions could be fully neutralized by NH_4^+ except in May; that is, other cations might affect the neutralization in May in addition to NH_4^+ . Thus, we calculated the correlations between

$([\text{NH}_4^+] + [\text{K}^+])$ and $([\text{NO}_3^-] + 2[\text{SO}_4^{2-}] + [\text{Cl}^-])$ in May, and found that the slope was 1.00, suggesting that K^+ was another cation that could strongly influence the neutralization of anions in $\text{PM}_{2.5}$. Comparatively, the result differed from that of Ningbo, where Ca^{2+} was found to be another cation affecting the neutralization [27].

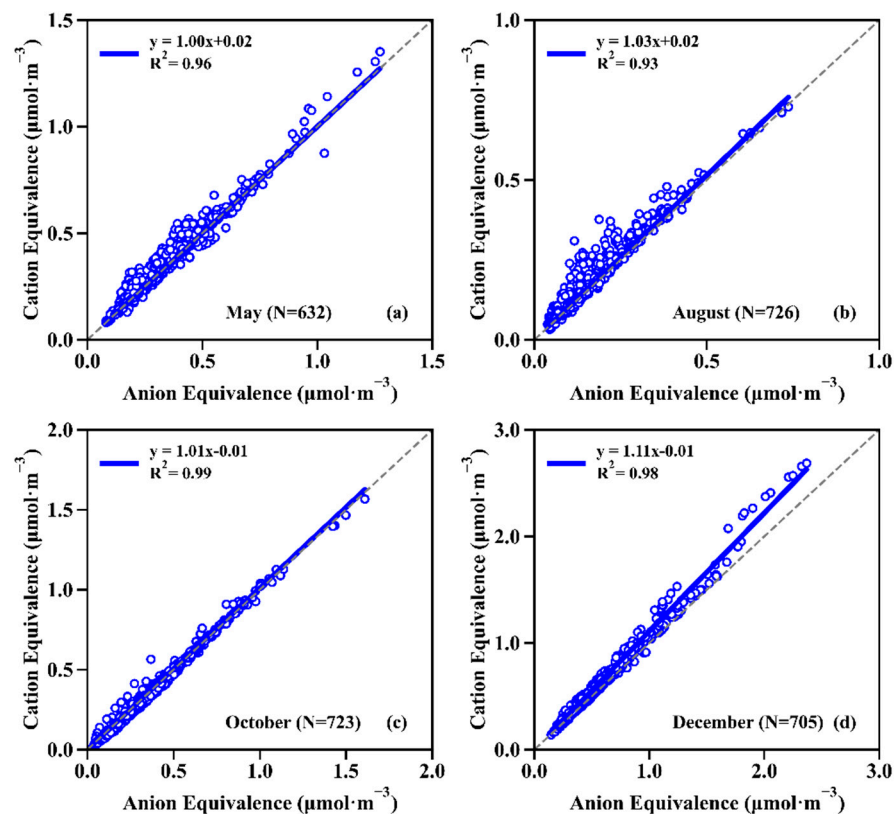


Figure 2. Scatter plots of cations equivalents (CE) versus anions equivalents (AE) in May (a), August (b), October (c) and (d) December.

3.4. Formations of Secondary Aerosols

Sulfur oxidation ratio (SOR) and nitrogen oxidation ratio (NOR) had been frequently used in previous studies to measure the degrees of oxidation of sulfur and nitrogen [27,35,52]. Higher SOR and NOR values could indicate a larger proportion of sulfate and nitrate formed by the secondary chemical reactions [53]. Thus, we calculated the values of the sulfur oxidation ratio (SOR) and nitrogen oxidation ratio (NOR) in four seasons for further investigating the transformation of SO_2 to sulfate and NO_2 to nitrate, respectively [53]:

$$(1) \quad \text{SOR} = \frac{[\text{SO}_4^{2-}]}{[\text{SO}_4^{2-}] + [\text{SO}_2]}$$

$$(2) \quad \text{NOR} = \frac{[\text{NO}_3^-]}{[\text{NO}_3^-] + [\text{NO}_2]}$$

Secondary transformations of SO_2 and NO_2 were dominant sources of sulfate and nitrate, respectively, when the values of SOR and NOR were >0.1 [54]. During the study period, the average values of SOR and NOR were 0.39 ± 0.13 and 0.15 ± 0.10 , with the highest values of 0.87 and 0.65, respectively. Mean values of SOR were 0.45 in May, 0.41 in August, 0.39 in October and 0.32 in December. Lower values of SOR in December may be due to lower temperature, since low temperature was an unfavorable factor for transformations of SO_2 to SO_4^{2-} [51]. Higher values of SOR in May and August were a result of higher solar radiation and temperature, which could enhance the reactions of SO_2 with OH radicals [27]. Mean values of NOR were 0.14 in May, 0.07 in August, 0.16 in October and 0.22 in December. NOR values showed the lowest value in August, although solar radiation was more favorable for the conversion of NO_2 to nitrate [54]. This may be

due the fact that nitrates (e.g., NH_4NO_3) can decompose into gaseous NH_3 and HNO_3 under higher temperatures in summer time [51].

3.5. Back Trajectory and Clusters Analysis

As shown in Figure 3 and Table 3, in May (Figure 3a), cluster 1 accounted for 9.70% of total air masses, mainly through the East China Sea and the southern part of Zhejiang province, carrying the highest concentrations of sulfate and $\text{PM}_{2.5}$. Industrial areas in the southern part of Zhejiang province (e.g., Ningbo) may have contributed to cluster 2 [55]. Cluster 2 accounted mostly for total air masses (41.08%) through the East China Sea and Zhejiang province, carrying the lowest $\text{PM}_{2.5}$ concentrations among the four clusters. 35.46% of air masses (cluster 3) came through Shandong and Jiangsu provinces, carrying the highest SNA before approaching Hangzhou. Cluster 3 passed through polluted and coastal areas, so moisture coming from the sea may have facilitated the secondary reactions of SO_2 and NO_2 [29]. Cluster 4 carried the lowest SNA concentrations through Hubei and Jiangxi provinces.

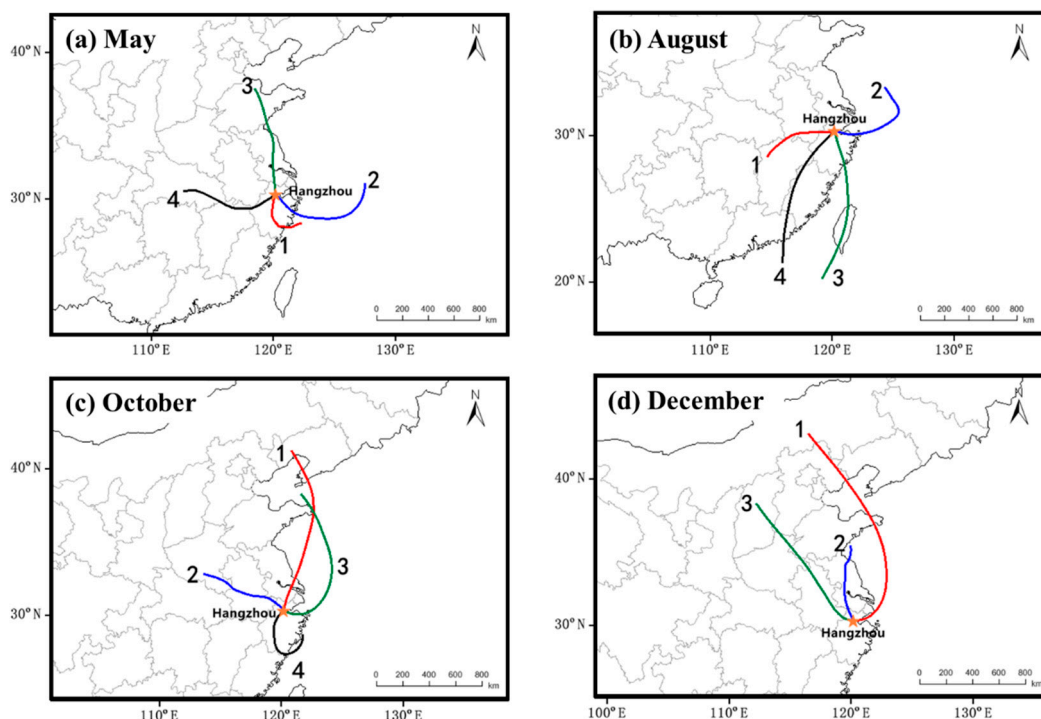


Figure 3. Clusters from 72 h backward trajectory analyses in May (a), August (b), October (c) and December (d) in 2017.

In August (Figure 3b), cluster 1 accounted for 24.53% of total air masses mainly through Jiangxi, Anhui provinces, carrying the highest concentrations of SNA and $\text{PM}_{2.5}$. Cluster 2 and cluster 3 accounted for 23.13% and 19.76% of total air masses which mainly passed the Yellow Sea and the South China Sea. Cluster 4 accounted for 32.56% of total air masses which mainly passed the South China Sea, Guangdong province and Fujian province, carrying the lowest concentrations of SNA and $\text{PM}_{2.5}$.

In October (Figure 3c), the air masses of cluster 1 (50.30%)—which originated from the Liaoning province passed through the Yellow Sea and Jiangsu province to reach the site—were dominated by the lower concentrations of $\text{PM}_{2.5}$ and SNA. Cluster 3, passing through the Yellow Sea and the Bohai Sea, accounted for 31.04% of total air masses. Air masses passing through Henan and Anhui provinces (cluster 2) and the southern region of Zhejiang province (cluster 4) carried the high concentrations of $\text{PM}_{2.5}$ and SNA and they accounted for a low percentage (18.68%) of the total air masses.

Table 3. Percentages of trajectories, mean concentrations of PM_{2.5}, SO₄^{2−}, NO₃[−] and NH₄⁺ for each trajectory cluster in May, August, October and December (see Figure 3).

Seasons	Cluster	Percents	Mean Concentration (µg·m ^{−3})					Main Area Passed by Air Masses
			PM _{2.5}	SNA	NO ₃ [−]	SO ₄ ^{2−}	NH ₄ ⁺	
May	1	9.70%	65.17 ± 19.92	22.24 ± 4.81	5.49 ± 1.77	11.03 ± 2.62	5.72 ± 1.26	Zhejiang province East China Sea,
	2	41.08%	53.91 ± 23.39	22.23 ± 10.62	8.63 ± 3.40	8.11 ± 5.60	5.49 ± 2.68	Zhejiang province Shandong,
	3	35.46%	64.65 ± 31.06	29.43 ± 16.68	11.85 ± 6.98	10.35 ± 7.79	7.23 ± 4.07	Jiangsu provinces Hubei, Jiangxi
	4	13.71%	57.75 ± 23.21	18.77 ± 8.55	4.28 ± 1.53	9.78 ± 3.92	4.71 ± 2.22	provinces
August	1	24.53%	39.27 ± 12.69	19.16 ± 9.32	4.87 ± 1.58	9.21 ± 4.12	5.08 ± 2.44	Jiangxi, Anhui provinces
	2	23.13%	32.74 ± 10.47	17.11 ± 4.62	5.64 ± 3.02	7.18 ± 2.77	4.29 ± 1.18	Yellow Sea
	3	19.76%	34.28 ± 7.63	9.96 ± 5.48	2.59 ± 0.96	4.72 ± 4.26	2.65 ± 1.52	South China Sea South China
	4	32.56%	30.96 ± 13.73	9.59 ± 6.36	2.64 ± 1.18	4.37 ± 3.14	2.58 ± 1.81	Sea; Guangdong, Fujian provinces
October	1	50.30%	44.85 ± 19.62	23.93 ± 15.73	10.84 ± 6.00	7.38 ± 3.82	5.71 ± 3.43	Liaoning, Jiangsu Provinces; Yellow Sea
	2	11.77%	75.33 ± 30.61	35.22 ± 21.51	17.80 ± 9.32	8.96 ± 8.05	8.46 ± 5.53	Henan, Anhui provinces
	3	31.04%	55.96 ± 23.76	27.01 ± 13.80	13.01 ± 7.97	7.34 ± 4.76	6.66 ± 3.87	Bohai Sea, Yellow Sea
	4	6.91%	82.44 ± 31.70	29.71 ± 16.34	13.47 ± 8.45	8.76 ± 4.75	7.48 ± 4.18	Zhejiang province
December	1	36.32%	78.42 ± 25.12	36.02 ± 10.30	17.71 ± 5.82	8.73 ± 2.32	9.58 ± 2.59	Inner Mongolia region, Hebei, Shandong provinces
	2	17.71%	81.00 ± 31.26	45.16 ± 27.86	22.16 ± 14.03	11.22 ± 6.97	11.78 ± 7.59	Jiangsu province
	3	46.02%	100.14 ± 43.05	41.02 ± 10.46	21.50 ± 6.00	9.10 ± 2.48	10.42 ± 2.98	Shanxi, Henan, Anhui provinces

In December (Figure 3d), the air masses originated from the northwest and southwest. Air masses of cluster 1 originated from the Inner Mongolia region, passing through Hebei and Shandong provinces with the lowest concentrations of SNA and PM_{2.5}. This was because cluster 1 mainly passed through the clean sea areas which caused the low PM_{2.5} level. Cluster 2, which came from Bohai Sea through the middle areas of Jiangsu province, carried the highest concentrations of SNA (45.16 µg·m^{−3}). Central areas of Jiangsu province were also found to be one of important potential sources areas for the winter haze event because of their high emissions [29,31,55]. Cluster 3 through Shanxi, Henan and Anhui provinces accounted for 46.02% of total air masses and carried the highest PM_{2.5} concentrations (100.14 µg·m^{−3}). Cluster 3 carried lower SNA concentrations than cluster 2 did, and this could be explained by the inland pathways of cluster 3 (i.e., less moisture than coastal pathway of cluster 2) [29].

3.6. PCA Analysis

PCA results are shown in Table 4. In May, the WSIs were mainly the result of two principal sources which constituted 56.55% of total variances. Component 1 accounted for 37.17% of total variance with very high loadings of SNA and K^+ , revealing that vehicle emissions, biomass burning, and secondary inorganic aerosols made significant contributions to $PM_{2.5}$ in May. Component 2 accounted for 19.38% of total variance with high loadings of Na^+ , Ca^+ , and Mg^{2+} , suggesting possible main contributions from sea salts and construction dusts.

Table 4. Results of the principal component analysis for WSIs in $PM_{2.5}$ in Hangzhou.

Season	May		August			October			December	
	Component		Component			Component			Component	
	1	2	1	2	3	1	2	3	1	2
NO_3^-	0.88	−0.01	0.86	−0.08	−0.18	0.93	−0.14	−0.18	0.90	−0.23
SO_4^{2-}	0.65	−0.30	0.92	−0.08	0.01	0.79	−0.45	0.07	0.82	−0.45
NH_4^+	0.92	−0.13	0.98	−0.11	−0.05	0.95	−0.25	−0.12	0.91	−0.37
Cl^-	0.20	−0.04	−0.11	−0.66	0.25	0.71	0.31	−0.18	0.65	0.16
K^+	0.69	0.38	0.82	0.07	0.24	0.04	−0.48	0.77	0.57	0.60
Na^+	0.55	0.59	0.07	0.69	−0.32	0.30	0.71	0.30	0.72	0.48
Ca^{2+}	−0.32	0.68	0.04	0.36	0.89	0.29	0.14	0.50	0.05	0.83
Mg^{2+}	−0.05	0.69	0.13	0.48	0.05	0.45	0.59	0.20	0.21	0.40
variance (%)	37.17	19.38	40.83	16.25	13.06	41.05	18.59	11.36	45.56	23.75
Cumulative (%)	37.17	56.55	40.83	57.08	70.14	41.05	59.64	71.00	45.56	69.31

Note: values in bold indicate loading factors discussed in this study.

In August, three principal components identified explain 70.14% of the total variance. Component 1 accounted for 40.83% of variance with high loadings of SNA and K^+ , revealing that the sources of secondary aerosols, vehicle emissions and biomass burning contributed notably in August. Component 2 with high loadings of Na^+ and Mg^{2+} could be attributed to sea salts. Component 3 accounted for 13.06% of total variance with a high loading of Ca^{2+} contributed from dusts of constructions.

In October, three main factors were obtained from the PCA model calculation. Component 1 accounted for 41.05% of total variance with high loadings of SNA and Cl^- , indicating major contributions from fossil fuel combustions, vehicle emissions and secondary aerosols. Component 2 accounted for 18.59% of total variance with high loadings of Na^+ and Mg^{2+} probably resulted from sea salt sources. Component 3 covered 11.36% of total variance with high loadings of K^+ and Ca^{2+} probably contributed by biomass burning and dusts.

In December, there were two major components which accounted for 69.31% of total variance. Component 1 accounting for 45.56% of total variance comprised SNA, Na^+ and Cl^- , suggesting the contributions from secondary aerosols, vehicle emissions and coal combustions. Component 2, accounting for 23.75% of variance with high loading of K^+ and Ca^{2+} , could be explained by contributions from biomass burning and dust from constructions.

4. Conclusions

To investigate potential sources and provide scientific insights into seasonal variations in the chemistry of WSIs (SO_4^{2-} , NO_3^- , NH_4^+ , Cl^- , Na^+ , K^+ , Ca^{2+} , Mg^{2+}) of $PM_{2.5}$ in Hangzhou, hourly concentrations of WSIs, as well as $PM_{2.5}$, NO_2 and SO_2 , were measured online at an urban site during four months (May, August, October and December) in 2017. The hourly concentrations of $PM_{2.5}$ during the whole campaign varied from 1 to $292 \mu g \cdot m^{-3}$ with the mean of $56.03 \mu g \cdot m^{-3}$, which exceeded Chinese National Ambient Air Quality Standard grade II ($35 \mu g \cdot m^{-3}$). The average concentration of WSIs was $26.49 \pm 20.78 \mu g \cdot m^{-3}$, which contributed 48.28% to $PM_{2.5}$ mass. SNA (SO_4^{2-} , NO_3^- and NH_4^+) were the most abundant ions in $PM_{2.5}$ and averagely comprised 41.57% of $PM_{2.5}$

during the observation. PM_{2.5}, NO₂, SO₂ and all WSIs showed higher concentrations in December among four sampling months, possibly due to higher emissions and unfavorable meteorological factors (e.g., lower wind speed and temperature). SOR and NOR were, on average, 0.39 ± 0.13 and 0.15 ± 0.10 , respectively, revealing that secondary transformations of SO₂ and NO₂ were dominant sources of sulfate and nitrate. Secondary aerosols and vehicle emissions were dominant sources of WSIs in Hangzhou based on the PCA analysis and regional transports of aerosols cannot be neglected. Thus, in the future, further controls on emissions of precursors of SNA (e.g., SO₂ and NO₂) should be implemented in Hangzhou. Moreover, emissions of industrial areas should be controlled at local and regional scales.

Author Contributions: S.Y. designed this study and X.C. and S.Y. wrote the manuscript. C.X. and S.Y. contributed to observations and data analyses, C.X., W.L., Z.L., Y.Z., M.L., W.L., P.L. and J.H.S. contributed to the discussions. S.Y. contributed to the manuscript and supervised the research. All authors have read and agreed to the published version of the manuscript.

Funding: This work was partially supported by the Department of Science and Technology of China (Nos. 2018YFC0213506, 2018YFC0213503, and 2016YFC0202702), National Research Program for Key Issues in Air Pollution Control in China (No. DQGG0107), and National Natural Science Foundation of China (Nos. 21577126 and 41561144004). Part of this work was also supported by the “Zhejiang 1000 Talent Plan” and Research Center for Air Pollution and Health in Zhejiang University. Pengfei Li is supported by National Natural Science Foundation of China (No. 22006030), Initiation Fund for Introducing Talents of Hebei Agricultural University (412201904), and Hebei Youth Top Q15 Fund (BJ2020032).

Institutional Review Board Statement: Not applicable.

Informed Consent Statement: Not applicable.

Data Availability Statement: Data that support the findings of this study are available from the corresponding author upon request.

Conflicts of Interest: The authors declare no conflict of interest.

References

1. Li, G.; Fang, C.; Wang, S.; Sun, S. The Effect of Economic Growth, Urbanization, and Industrialization on Fine Particulate Matter (PM_{2.5} Concentrations in China. *Environ. Sci. Technol.* **2016**, *50*, 11452–11459. [\[CrossRef\]](#)
2. Zhao, H.; Guo, S.; Zhao, H. Characterizing the influences of economic development, energy consumption, urbanization, industrialization, and vehicles amount on PM_{2.5} concentrations of China. *Sustainability* **2018**, *10*, 2574. [\[CrossRef\]](#)
3. Wang, X.; Tian, G.; Yang, D.; Zhang, W.; Lu, D.; Liu, Z. Responses of PM_{2.5} pollution to urbanization in China. *Energy Policy* **2018**, *123*, 602–610. [\[CrossRef\]](#)
4. Yang, D.; Chen, Y.; Miao, C.; Liu, D. Spatiotemporal variation of PM_{2.5} concentrations and its relationship to urbanization in the Yangtze river delta region, China. *Atmos. Pollut. Res.* **2020**, *11*, 491–498. [\[CrossRef\]](#)
5. Lu, X.; Lin, C.; Li, W.; Chen, Y.; Huang, Y.; Fung, J.C.H.; Lau, A.K.H. Analysis of the adverse health effects of PM_{2.5} from 2001 to 2017 in China and the role of urbanization in aggravating the health burden. *Sci. Total Environ.* **2019**, *652*, 683–695. [\[CrossRef\]](#) [\[PubMed\]](#)
6. Feng, S.; Gao, D.; Liao, F.; Zhou, F.; Wang, X. The health effects of ambient PM_{2.5} and potential mechanisms. *Ecotoxicol. Environ. Saf.* **2016**, *128*, 67–74. [\[CrossRef\]](#) [\[PubMed\]](#)
7. Pui, D.Y.H.; Chen, S.C.; Zuo, Z. PM_{2.5} in China: Measurements, sources, visibility and health effects, and mitigation. *Particuology* **2014**, *13*, 1–26. [\[CrossRef\]](#)
8. Han, L.; Zhou, W.; Li, W.; Li, L. Impact of urbanization level on urban air quality: A case of fine particles (PM_{2.5} in Chinese cities. *Environ. Pollut.* **2014**, *194*, 163–170. [\[CrossRef\]](#) [\[PubMed\]](#)
9. Xu, X.; Zhang, T. Spatial-temporal variability of PM_{2.5} air quality in Beijing, China during 2013–2018. *J. Environ. Manag.* **2020**, *262*, 110263. [\[CrossRef\]](#) [\[PubMed\]](#)
10. Tagaris, E.; Liao, K.J.; Delucia, A.J.; Deck, L.; Amar, P.; Russell, A.G. Potential impact of climate change on air pollution-related human health effects. *Environ. Sci. Technol.* **2009**, *43*, 4979–4988. [\[CrossRef\]](#)
11. Tai, A.P.K.; Mickley, L.J.; Jacob, D.J. Correlations between fine particulate matter (PM_{2.5} and meteorological variables in the United States: Implications for the sensitivity of PM_{2.5} to climate change. *Atmos. Environ.* **2010**, *44*, 3976–3984. [\[CrossRef\]](#)
12. Wang, Y.; Gao, W.; Wang, S.; Song, T.; Gong, Z.; Ji, D.; Wang, L.; Liu, Z.; Tang, G.; Huo, Y.; et al. Contrasting trends of PM_{2.5} and surface-ozone concentrations in China from 2013 to 2017. *Natl. Sci. Rev.* **2020**, *7*, 1331–1339. [\[CrossRef\]](#) [\[PubMed\]](#)

13. Xue, W.; Zhang, J.; Zhong, C.; Ji, D.; Huang, W. Satellite-derived spatiotemporal PM_{2.5} concentrations and variations from 2006 to 2017 in China. *Sci. Total Environ.* **2020**, *712*, 134577. [CrossRef]
14. Zhao, L.; Wang, L.; Tan, J.; Duan, J.; Ma, X.; Zhang, C.; Ji, S.; Qi, M.; Lu, X.; Wang, Y.; et al. Changes of chemical composition and source apportionment of PM_{2.5} during 2013–2017 in urban Handan, China. *Atmos. Environ.* **2019**, *206*, 119–131. [CrossRef]
15. Zhao, C.; Niu, M.; Song, S.; Li, J.; Su, Z.; Wang, Y.; Gao, Q.; Wang, H. Serum metabolomics analysis of mice that received repeated airway exposure to a water-soluble PM_{2.5} extract. *Ecotoxicol. Environ. Saf.* **2019**, *168*, 102–109. [CrossRef]
16. Liu, H.; Tian, H.; Zhang, K.; Liu, S.; Cheng, K.; Yin, S.; Liu, Y.; Liu, X.; Wu, Y.; Liu, W.; et al. Seasonal variation, formation mechanisms and potential sources of PM_{2.5} in two typical cities in the Central Plains Urban Agglomeration, China. *Sci. Total Environ.* **2019**, *657*, 657–670. [CrossRef]
17. Wang, J.; Li, X.; Zhang, W.; Jiang, N.; Zhang, R.; Tang, X. Secondary PM_{2.5} in Zhengzhou, China: Chemical Species Based on Three Years of Observations. *Aerosol Air Qual. Res.* **2017**, *16*, 91–104. [CrossRef]
18. Jiang, N.; Guo, Y.; Wang, Q.; Kang, P.; Zhang, R.; Tang, X. Chemical Composition Characteristics of PM_{2.5} in Three Cities in Henan, Central China. *Aerosol Air Qual. Res.* **2017**, *17*, 2367–2380. [CrossRef]
19. Huang, X.; Liu, Z.; Zhang, J.; Wen, T.; Ji, D.; Wang, Y. Seasonal variation and secondary formation of size-segregated aerosol water-soluble inorganic ions during pollution episodes in Beijing. *Atmos. Res.* **2016**, *168*, 70–79. [CrossRef]
20. Zhang, F.; Wang, Z.W.; Cheng, H.R.; Lv, X.P.; Gong, W.; Wang, X.M.; Zhang, G. Seasonal variations and chemical characteristics of PM_{2.5} in Wuhan, central China. *Sci. Total Environ.* **2015**, *518*–519, 97–105. [CrossRef]
21. Shen, Z.; Cao, J.; Arimoto, R.; Han, Z.; Zhang, R.; Han, Y.; Liu, S.; Okuda, T.; Nakao, S.; Tanaka, S. Ionic composition of TSP and PM_{2.5} during dust storms and air pollution episodes at Xi'an, China. *Atmos. Environ.* **2009**, *43*, 2911–2918. [CrossRef]
22. Yu, S.; Zhang, Q.; Yan, R.; Wang, S.; Li, P.; Chen, B.; Liu, W.; Zhang, X. Origin of air pollution during a weekly heavy haze episode in Hangzhou, China. *Environ. Chem. Lett.* **2014**, *12*, 543–550. [CrossRef]
23. Zhou, M.; Zhang, Y.; Han, Y.; Wu, J.; Du, X.; Xu, H.; Feng, Y.; Han, S. Spatial and temporal characteristics of PM_{2.5} acidity during autumn in marine and coastal area of Bohai Sea, China, based on two-site contrast. *Atmos. Res.* **2018**, *202*, 196–204. [CrossRef]
24. Xue, J.; Lau, A.K.H.; Yu, J.Z. A study of acidity on PM_{2.5} in Hong Kong using online ionic chemical composition measurements. *Atmos. Environ.* **2011**, *45*, 7081–7088. [CrossRef]
25. Zhang, G.; Xu, H.; Qi, B.; Du, R.; Gui, K.; Wang, H.; Jiang, W.; Liang, L.; Xu, W. Characterization of atmospheric trace gases and particulate matter in Hangzhou, China. *Atmos. Chem. Phys.* **2018**, *18*, 1705–1728. [CrossRef]
26. Hangzhou Municipal People's Government Home Page. Available online: <http://www.hangzhou.gov.cn/> (accessed on 29 July 2021).
27. Xu, J.S.; He, J.; Behera, S.N.; Xu, H.H.; Ji, D.S.; Wang, C.J.; Yu, H.; Xiao, H.; Jiang, Y.J.; Qi, B.; et al. Temporal and spatial variation in major ion chemistry and source identification of secondary inorganic aerosols in Northern Zhejiang Province, China. *Chemosphere* **2017**, *179*, 316–330. [CrossRef]
28. Liu, G.; Li, J.; Wu, D.; Xu, H. Chemical composition and source apportionment of the ambient PM_{2.5} in Hangzhou, China. *Particuology* **2015**, *18*, 135–143. [CrossRef]
29. Wu, J.; Xu, C.; Wang, Q.; Cheng, W. Potential sources and formations of the PM_{2.5} pollution in urban Hangzhou. *Atmosphere* **2016**, *7*, 100. [CrossRef]
30. Chen, K.; Metcalfe, S.E.; Yu, H.; Xu, J.; Xu, H.; Ji, D.; Wang, C.; Xiao, H.; He, J. Characteristics and source attribution of PM_{2.5} during 2016 G20 Summit in Hangzhou: Efficacy of radical measures to reduce source emissions. *J. Environ. Sci.* **2021**, *106*, 47–65. [CrossRef]
31. Hua, Y.; Cheng, Z.; Wang, S.; Jiang, J.; Chen, D.; Cai, S.; Fu, X.; Fu, Q.; Chen, C.; Xu, B.; et al. Characteristics and source apportionment of PM_{2.5} during a fall heavy haze episode in the Yangtze River Delta of China. *Atmos. Environ.* **2015**, *123*, 380–391. [CrossRef]
32. Jansen, R.C.; Shi, Y.; Chen, J.; Hu, Y.J.; Xu, C.; Hong, S.; Li, J.; Zhang, M. Using hourly measurements to explore the role of secondary inorganic aerosol in PM_{2.5} during haze and fog in Hangzhou, China. *Adv. Atmos. Sci.* **2014**, *31*, 1427–1434. [CrossRef]
33. Cheng, M.C.; You, C.F.; Cao, J.; Jin, Z. Spatial and seasonal variability of water-soluble ions in PM_{2.5} aerosols in 14 major cities in China. *Atmos. Environ.* **2012**, *60*, 182–192. [CrossRef]
34. Chang, M.; Sioutas, C.; Cassee, F.; Fokkens, P.H. Field evaluation of a mobile high-capacity particle size classifier (HCPSC) for separate collection of coarse, fine and ultrafine particles. *J. Aerosol Sci.* **2001**, *32*, 139–156. [CrossRef]
35. Khezri, B.; Mo, H.; Yan, Z.; Chong, S.-L.; Heng, A.K.; Webster, R.D. Simultaneous online monitoring of inorganic compounds in aerosols and gases in an industrialized area. *Atmos. Environ.* **2013**, *80*, 352–360. [CrossRef]
36. Rumsey, I.C.; Cowen, K.A.; Walker, J.T.; Kelly, T.J.; Hanft, E.A.; Mishoe, K.; Rogers, C.; Proost, R.; Beachley, G.M.; Lear, G.; et al. An assessment of the performance of the Monitor for AeRosols and Gases in ambient air (MARGA): A semi-continuous method for soluble compounds. *Atmos. Chem. Phys.* **2014**, *14*, 5639–5658. [CrossRef]
37. Xu, L.; Chen, X.; Chen, J.; Zhang, F.; He, C.; Zhao, J.; Yin, L. Seasonal variations and chemical compositions of PM_{2.5} aerosol in the urban area of Fuzhou, China. *Atmos. Res.* **2012**, *104*–105, 264–272. [CrossRef]
38. Wang, S.; Yu, S.; Li, P.; Wang, L.; Mehmood, K.; Liu, W.; Yan, R.; Zheng, X. A study of characteristics and origins of haze pollution in Zhengzhou, China, based on observations and hybrid receptor models. *Aerosol Air Qual. Res.* **2017**, *17*, 513–528. [CrossRef]

39. Gao, X.; Yang, L.; Cheng, S.; Gao, R.; Zhou, Y.; Xue, L.; Shou, Y.; Wang, J.; Wang, X.; Nie, W.; et al. Semi-continuous measurement of water-soluble ions in PM_{2.5} in Jinan, China: Temporal variations and source apportionments. *Atmos. Environ.* **2011**, *45*, 6048–6056. [[CrossRef](#)]
40. Abdalmogith, S.S.; Harrison, R.M. The use of trajectory cluster analysis to examine the long-range transport of secondary inorganic aerosol in the UK. *Atmos. Environ.* **2005**, *39*, 6686–6695. [[CrossRef](#)]
41. Sun, W.; Sun, J. Daily PM_{2.5} concentration prediction based on principal component analysis and LSSVM optimized by cuckoo search algorithm. *J. Environ. Manag.* **2017**, *188*, 144–152. [[CrossRef](#)]
42. Song, Y.; Xie, S.; Zhang, Y.; Zeng, L.; Salmon, L.G.; Zheng, M. Source apportionment of PM_{2.5} in Beijing using principal component analysis/absolute principal component scores and UNMIX. *Sci. Total Environ.* **2006**, *372*, 278–286. [[CrossRef](#)]
43. Guo, W.; Long, C.; Zhang, Z.; Zheng, N.; Xiao, H.; Xiao, H. Seasonal control of water-soluble inorganic ions in PM_{2.5} from nanning, a subtropical monsoon climate city in southwestern China. *Atmosphere* **2020**, *11*, 5. [[CrossRef](#)]
44. Xiao, K.; Wang, Y.; Wu, G.; Fu, B.; Zhu, Y. Spatiotemporal Characteristics of Air Pollutants (PM₁₀, PM_{2.5}, SO₂, NO₂, O₃, and CO in the Inland Basin City of Chengdu, Southwest China. *Atmosphere* **2018**, *9*, 74. [[CrossRef](#)]
45. Rahman, A.; Luo, C.; Khan, M.H.R.; Ke, J.; Thilakanayaka, V.; Kumar, S. Influence of atmospheric PM_{2.5}, PM₁₀, O₃, CO, NO₂, SO₂, and meteorological factors on the concentration of airborne pollen in Guangzhou, China. *Atmos. Environ.* **2019**, *212*, 290–304. [[CrossRef](#)]
46. Wang, S.; Yu, S.; Yan, R.; Zhang, Q.; Li, P.; Wang, L.; Liu, W.; Zheng, X. Characteristics and origins of air pollutants in Wuhan, China, based on observations and hybrid receptor models. *J. Air Waste Manag. Assoc.* **2017**, *67*, 739–753. [[CrossRef](#)]
47. Wang, Y.; Ying, Q.; Hu, J.; Zhang, H. Spatial and temporal variations of six criteria air pollutants in 31 provincial capital cities in China during 2013–2014. *Environ. Int.* **2014**, *73*, 413–422. [[CrossRef](#)]
48. He, Q.; Yan, Y.; Guo, L.; Zhang, Y.; Zhang, G.; Wang, X. Characterization and source analysis of water-soluble inorganic ionic species in PM_{2.5} in Taiyuan city, China. *Atmos. Res.* **2017**, *184*, 48–55. [[CrossRef](#)]
49. Li, M.; Li, C.; Zhang, M. Exploring the spatial spillover effects of industrialization and urbanization factors on pollutants emissions in China's Huang-Huai-Hai region. *J. Clean. Prod.* **2018**, *195*, 154–162. [[CrossRef](#)]
50. Duan, F.; Liu, X.; Yu, T.; Cachier, H. Identification and estimate of biomass burning contribution to the urban aerosol organic carbon concentrations in Beijing. *Atmos. Environ.* **2004**, *38*, 1275–1282. [[CrossRef](#)]
51. Yin, L.; Niu, Z.; Chen, X.; Chen, J.; Zhang, F.; Xu, L. Characteristics of water-soluble inorganic ions in PM_{2.5} and PM_{2.5–10} in the coastal urban agglomeration along the Western Taiwan Strait Region, China. *Environ. Sci. Pollut. Res.* **2014**, *21*, 5141–5156. [[CrossRef](#)] [[PubMed](#)]
52. Zhang, T.; Cao, J.J.; Tie, X.X.; Shen, Z.X.; Liu, S.X.; Ding, H.; Han, Y.M.; Wang, G.H.; Ho, K.F.; Qiang, J.; et al. Water-soluble ions in atmospheric aerosols measured in Xi'an, China: Seasonal variations and sources. *Atmos. Res.* **2011**, *102*, 110–119. [[CrossRef](#)]
53. Wu, X.; Xu, L.; Hong, Y.; Chen, J.; Qiu, Y.; Hu, B.; Hong, Z.; Zhang, Y.; Liu, T.; Chen, Y.; et al. The air pollution governed by subtropical high in a coastal city in Southeast China: Formation processes and influencing mechanisms. *Sci. Total Environ.* **2019**, *692*, 1135–1145. [[CrossRef](#)] [[PubMed](#)]
54. Zhang, R.; Sun, X.; Shi, A.; Huang, Y.; Yan, J.; Nie, T.; Yan, X.; Li, X. Secondary inorganic aerosols formation during haze episodes at an urban site in Beijing, China. *Atmos. Environ.* **2018**, *177*, 275–282. [[CrossRef](#)]
55. Zhang, Q.; Yan, R.; Fan, J.; Yu, S.; Yang, W.; Li, P.; Wang, S.; Chen, B.; Liu, W.; Zhang, X. A heavy haze episode in Shanghai in december of 2013: Characteristics, origins and implications. *Aerosol Air Qual. Res.* **2015**, *15*, 1881–1893. [[CrossRef](#)]